A Novel Way To Design Suitable Inorganic Material from the Smectite Family for Sorption of 2,3,7,8-Tetrachlorinated Dibenzo-p-dioxin

ARTICLE *in* THE JOURNAL OF PHYSICAL CHEMISTRY A · FEBRUARY 2000

Impact Factor: 2.69 · DOI: 10.1021/jp9936704

3 AUTHORS:

Abhijit Chatterjee
BIOVIA
87 PUBLICATIONS **1,131** CITATIONS
SEE PROFILE

Takashi Iwasaki
National Institute of Advanced Industrial Sc…
59 PUBLICATIONS **626** CITATIONS
SEE PROFILE

Takeo Ebina
National Institute of Advanced Industrial Sc…
142 PUBLICATIONS **1,539** CITATIONS
SEE PROFILE

2,3,7,8-テトラクロロジベンゾ-*p*-ジオキシンの吸着に適した無機材料をスメクタイト群から設計する新規な方法*1

A. Chatterjee*2、岩崎孝志*3、蛯名武雄*4

A Novel Way to Design Suitable Inorganic Materials from the Smectite Family for Sorption of 2,3,7,8-Tetrachlorinated Dibenzo-*p*-dioxin

A. Chatterjee, T. Iwasaki, T. Ebina

The activities of 2,3,7,8-tetrachlorinated dibenzo-*p*-dioxin (2,3,7,8-TCDD), a highly toxic pollutant, and its suitable sorbent from the dioctahedral smectite family are investigated using a range of reactivity indexes using density functional theory (DFT). From the values of the local softness and the charge on the hydrogen atom of the bridging hydroxyl attached to the octahedral metal site present in smectite, used as a first approximation to the local hardness, it is concluded that the local acidities of the inorganic material systems are dependent on several characteristics which are of importance within the framework of the hard and soft acids and bases principle. We first rationalized an understanding of the electronic structure of 2,3,7,8-TCDD, followed by the local softness calculation, to locate its active site. We compared its activity with that of the OH group of the isomorphously substituted (Fe^{3+}, Mg^{2+}, Fe^{2+}, and Li^{+}) dioctahedral smectite family. The recently proposed local hard−soft acid−base principle characterizes the reactive centers of two systems on the basis of equal local softness. We validate the proposition by considering the interaction between systems with different global softnesses, which further paves the way for proposing a novel qualitative way to choose the best sorption material. The results were compared with the interaction energy calculations using DFT. The ordering for best sorption follows the order $Mg^{2+} > Fe^{2+} > Fe^{3+} > Li^{+}$.

Introduction

Polychlorinated dibenzo-*p*-dioxins (PCDDs), highly toxic materials, have been detected as trace contaminants in incinerator fly ash,[1] herbicide formulations, and the synthesis of several important commercial chlorophenolic compunds.[2] In recent years a number of poisoning fears have been generated because of release of these substances into the environment.[3] Among 75 possible PCDDs containing one to eight possible chlorine substitutions, 2,3,7,8-tetrachlorodibenzo-*p*-dioxin (2,3,7,8-TCDD) shows the highest degree of toxicity.[4] This has triggered a large number of studies,[5] both experimental and theoretical, aimed at elucidating the chemical and biological properties of TCDD-related compounds. Experimental information about the molecular parameters if dioxin is hard to obtain because of its high toxicity. Molecular orbital calculations can be used to provide vital information about these molecules, in the absence of experimental data.

There are many theoretical studies on PCDD; most of them are empirical with few exceptions. A computational force field MMP2 was employed to derive molecular geometries of some PCDDs.[6] Makino et al.[7] have reported a photodegradation mechanism of PCDDs, without any comments on the geometrical parameters. A MNDO study, which calculated the physical properties such as heat of formation, ionization potentials, and dipole moments of many PCDDs, has been reported.[8] Here also the geometries and structures were not mentioned. A few ab initio studies were also performed with PCDDs without much information about the energetics.[9,10]

The mechanism of the toxicity attributed to the PCDDs depends on structurally related properties.[11] From that point of view, molecular geometry and conformational and stereoelectronic features such as planarity, dipole moment, and polarizability are essential subjects to investigate. Fujii et al.[12] have studied the structure and energy of TCDD using Gaussian 92, which does not talk about the active site of the TCDD. Without knowledge of the active site of the toxic molecule, it is difficult to find its suitable sorbent. Now, active site means the site that is reactive to other material, which will actively take part in the bond breaking and making process. Because of the high toxicity of TCDD, the best choice of its elimination from the environment is preconcentration, which is discussed in the following section. We used the work of Fujii et al.[12] as the reference to validate our results about the structural parameters obtained using density functional theory (DFT).

Now, to destroy dioxin by biological, chemical, or thermal means involves high costs, because it occurs in such low concentrations in the environment. Because of its high toxicity, there is no lower limit at which dioxin can be considered safe and would therefore require no remedial action. The concentration can be achieved through adsorption of the dioxin from solution onto a solid.[13] The optimal solid sorbent for dioxin should have the following properties: low cost, ease of handling, environmental neutrality, high affinity, high selectivity, and capability of being integrated into a dioxin-destruction process. Among the many candidates examined experimentally, clays met the majority of the above criteria; however, clays in their natural state exhibit neither a high affinity for nor removal selectivity of hydrophobic compounds, such as dioxin.[14,15] Nolan et al.[16,17] have developed an inorganic clay (hydroxy-Al-montmorillonite) and an organoclay (humic acid−hydroxy-Al-montmorillonite). The high bonding affinity of the former for dioxin was attributed to the clay's ability to function as a two-dimensional zeolite. Boyd and Mortland[18] have shown that

*1 This paper was reprinted from The Journal of Physical Chemistry A, Vol.104, No.10, pp.2098-2104, with permission of American Chemical Society.
*2 Domestic Research Fellowship
*3 Director of Research Planning Division
*4 Inorganic Materials Section

Cu^{2+}-exchanged smectite catalyzes dioxin-dechlorination reactions. We want to explore the isomorphously substituted smectites to probe their activity toward dioxin and will propose a novel scale for choosing a particular clay without tedious experimentation. Bailey[19] has shown that monoclinic dioctahedral mica has two independent types of octahedra. The two OH groups of each octahedra lie on the symmetry plane of each layer: for the first octahedra it lies in the trans orientation and in the second case it lies at the cis position. Now in the case of smectites the activity solely lies on the orientation of the hydroxyl hydrogen attached to the octahedral aluminun present in 2:1 dioctahedral smectite. Sposito et al. pointed out that in the case of dioctahedral clays the OH bond is directed parallel to the clay sheet, with the hydrogen pointing to the octahedral vacancy.[20] This OH bond may act as the active site for molecular adsorption, as proposed by Delville.[21] He has modeled the clay–water interactions and shown that the water molecules form a hydrogen bond with the lone pair of the oxygen at the center of the hexagonal cavity. This is possible for dioctahedral clays, because the proton is directed parallel to the plane of the clay. There are suggestions from electrostatic calculations[22] that the orientations of these hydroxyl groups are sensitive to the octahedral cation plane at the center of the clay layer. Because these hydroxyl groups may be expected to play a major role in the catalytic activity of 2:1 clays and their interaction with water and other polar molecules, it is important to examine their orientation more closely. We therefore want to explore the role of this hydroxyl hydrogen with isomorphous substitution and will probe the stability of the adsorption complex of dioxin with the smectite surface. We want to emphasize the interaction between the active site of the dioctahedral clay, which is the hydroxyl group present in the octahedral layer of the clay, and the active site of the TCDD molecule because this will play a key role in the sorption of the dioxin molecule on clay matrixes.

So far there are many experimental and theoretical studies to monitor the interaction of molecules with a clay surface, but there is no effort so far to correlate the activity of the molecules in terms of the interaction with a clay surface. Now, the hard–soft acid–base (HSAB) principles classify the interaction between acids and bases in terms of global softness. Pearson proposed the global HSAB principle.[23] The global hardness was defined[23] as the second derivative of energy with respect to the number of electrons at constant temperature and external potential, which includes the nuclear field. The global softness is the inverse of this.[23] Pearson also suggested a principle of maximum hardness (PMH),[24] which states that, for a constant external potential, the system with the maximum global hardness is most stable. In recent days, DFT has gained widespread use in quantum chemistry. Some DFT-based local properties, e.g., Fukui functions and local softness,[25] have already been used for reliable predictions in various types of electrophilic and nucleophilic reactions.[26–29] In our recent study[30] we proposed a reactivity index scale for heteroatomic interaction with a zeolite framework. Moreover, Gazquez and Mendez[31] proposed that when two molecules A and B of equal softness interact, thereby implicitly assuming one of the species as nucleophile and the other as an electrophile, then a novel bond would likely form between an atom of A and an atom of B, whose Fukui function values are close to each other.

In the present study we first use DFT-based local reactivity descriptors to correlate the activity of 2,3,7,8-TCDD with different isomorphously substituted (Fe^{3+}, Mg^{2+}, Fe^{2+}, and Li^{+}) dioctahedral smectite surfaces. A cluster model was generated from the crystal structure of dioctahedral smectite montmorillonite, which is considered to reproduce and compare the effect of environment on the activity of the active center present in the clay surface. The reactivity indexes of nucleophilic and electrophilic sites were compared. An activity order was proposed. The results were compared with the interaction energy calculations with each of the isomorphously substituted clay clusters using DFT. A scale of activity is proposed in terms of the reactivity index, which paves a novel way of designing new material for a particular reaction of environmental importance.

Theory

Let us first recall the definition of various quantities employed. The Fukui function $f(r)$ is defined by[25]

$$f(r) = [\delta\mu/\delta v(r)]_N = [\delta\rho(r)/\delta N]_v \quad (1)$$

The function f is thus a local quantity, which has different values at different points in the species, N is the total number of electrons, μ is the chemical potential and v is the potential acting on an electron due to all nuclei present. Because $\rho(r)$ as a function of N has slope discontinuities, eq 1 provides the following three reaction indexes:[25]

$$f^-(r) = [\delta\rho(r)/\delta N]_v \quad \text{(governing electrophilic attack)}$$

$$f^+(r) = [\delta\rho(r)/\delta N]_v \quad \text{(governing nucleophilic attack)}$$

$$f^0(r) = \frac{1}{2}[f^+(r) + f^-(r)] \quad \text{(for radial attack)}$$

In a finite difference approximation, the condensed Fukui functions[32] of an atom, say x, in a molecule with N electrons are defined as

$$f_x^+ = [q_x(N+1) - q_x(N)] \quad \text{(for nucleophilic attack)}$$

$$f_x^- = [q_x(N) - q_x(N-1)] \quad \text{(for electrophilic attack)}$$

$$f_x^0 = [q_x(N+1) - q_x(N-1)]/2 \quad \text{(for radical attack)} \quad (2)$$

where q_x is the electronic population of atom x in a molecule. In DFT, hardness (η) is defined as[33]

$$\eta = \frac{1}{2}(\delta^2 E/\delta N^2)v(r) = \frac{1}{2}(\delta\mu/\delta N)v$$

The global softness, S, is defined as the inverse of the global hardness, η.

$$S = {}^1/_2\eta = (\delta N/\delta\mu)v$$

The local softness $s(r)$ can be defined as

$$s(r) = (\delta\rho(r)/\delta\mu)v \quad (3)$$

Equation 3 can also be written as

$$s(r) = [\delta\rho(r)/\delta N]v[\delta N/\delta\mu]v = f(r)\,S \quad (4)$$

Thus, local softness contains the same information as the Fukui function $f(r)$ plus additional information about the total molecular softness, which is related to the global reactivity with respect to a reaction partner, as stated in the HSAB principle. Using the finite difference approximation, S can be approximated as

$$S = 1/(\mathrm{IE} - \mathrm{EA}) \quad (5)$$

where IE and EA are the first ionization energy and electron affinity of the molecule, respectively. Atomic softness values can easily be calculated by using eq 4, namely

$$s_x^+ = [q_x(N+1) - q_x(N)]S$$

$$s_x^- = [q_x(N) - q_x(N-1)]S$$

$$s_x^0 = S[q_x(N+1) - q_x(N-1)]/2 \quad (6)$$

Computational Methodology and Models

In the present study, all calculations have been carried out with DFT[34] using DMOL code of MSI Inc. BLYP[35,36] exchange correlation functional and DNP basis set[37] were used throughout the calculation. BLYP has already shown its credibility for explaining weak hydrogen bond type interactions in comparison to MP2 level calculations.[38,39] It is also useful in describing the interaction of heteroatomic molecules with a zeolite framework cluster.[30] Basis set superposition error (BSSE) was also calculated for the current basis set in a nonlocal density approximation (NLDA) using the Boys–Bernardi method.[40] Geometries of the interacting molecule 2,3,7,8-TCDD along with the individual clay cluster models representing different isomorphous substitutions in the octahedral aluminum of dioctahedral smectites were fully optimized for calculating the reactivity index. The theory of reactivity index calculations is mentioned elsewhere in detail.[30] Single-point calculations of the cation and anion of each molecule at the optimized geometry of the neutral molecule were also carried out to evaluate Fukui functions and global and local softnesses. The condensed Fukui function and atomic softness were evaluated using eqs 2 and 6, respectively. The gross atomic charges were evaluated by using the technique of electrostatic potential (ESP) driven charges. It is well-known that Mulliken charges are highly basis set dependent, whereas ESP-driven charges show less basis set dependence[30,41,42] and are better descriptors of the molecular electronic density distribution. The ideal formula of the clay montmorillonite, a member of the 2:1 dioctahedral smectite family, is $(Na^+_x, nH_2O)(Al_{4-x}Mg_x)$-$Si_8O_{20}(OH)_4$.[43] The $Al_2Si_6O_{24}H_{18}$ cluster was generated from the clay structure as shown in Figure 1. Figure 1 displays the top view of one tetrahedral sheet and one octahedral sheet, showing the hexagonal cavities at the oxygen surface of the silicon layers. The dangling bonds were saturated with hydrogens, not shown in Figure 1 for visual clarity. The hydroxyl group at the center of the hexagonal cavity is parallel to the clay surface and pointing in the direction of the vacancy of the octahedral network. Of the two octahedral aluminums, one is more stable than the other, as reported in our earlier study.[43] Therefore, to mimic the isomorphous substitution, calculations were performed on a cluster model with formula $TSi_4O_{16}H_{10}$, where T = Fe^{3+}, Mg^{2+}, Fe^{2+}, and Li^+. The adjacent silicon and aluminum atoms occurring in the clay lattice are replaced by hydrogens to preserve the electroneutrality of the model as shown in Figure 2. The substitution energy was calculated for the most active aluminum between the two, by the following equation as mentioned in our earlier study.[44]

$$AlSi_4O_{16}H_{10} + TO_4^- \rightarrow TSi_4O_{16}H_{10} + AlO_4^-$$

Results and Discussion

The electronic and structural properties of 2,3,7,8-TCDD along with the clay cluster models are first rationalized. The relevant geometry results are presented in Table 1 for 2,3,7,8-TCDD. The values of nucleophilic condensed local softness (s_x^-) and condensed Fukui function (f_x^-) of the individual atoms of the TCDD obtained through the ESP technique at the DFT level are shown in Table 2. The substitution energies calculated for the clay cluster models are presented in Table 3. The global softness values of the clay cluster models as well as the interacting molecule calculated using DFT are presented in Table 4. The values of electrophilic condensed local softness (s_x^+) and condensed Fukui function (f_x^+) of the individual atoms of the cluster models obtained through the ESP technique at the DFT level are shown in Table 5. It is observed from Table 4 that those global softness values for the clay cluster models are lower than that of the interacting molecular species. So, to test the HSAB principle, it seems to be important to analyze whether the local softness values, Fukui functions, or reactive indexes for the constituent atoms of the cluster models and interacting molecular species will be the more reliable parameter. First, the interaction of all of the clay cluster models containing different isomorphous substituent cations with 2,3,7,8-TCDD is calculated using local softness values and an activity order is proposed. This order is validated by the interaction energy calculations. The orientation of the optimized TCDD conformation is also monitored to justify its interaction with hydroxyl hydrogen attached with octahedral alumina of the clay framework.

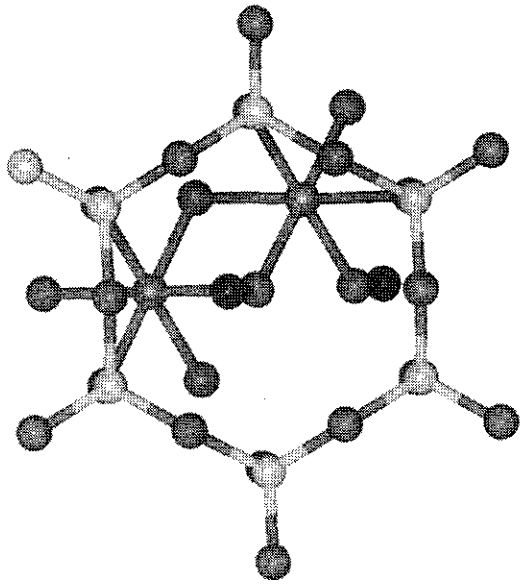

Figure 1. Cluster model of montmorillonite with six tetrahedral silicons and two octahedral aluminums. It is the top view of the cluster. The color code is as follows: red, oxygen; yellow, silicon; violet, octahedral aluminum; blue, hydroxyl hydrogen.

a. Structure, Electronic Properties, and Reactivity Indexes of an Isomorphously Substituted Clay Cluster. Isomorphous substitution of an Al^{3+} ion at an octahedral site by Li^+, Mg^{2+}, Fe^{2+}, and Fe^{3+} was treated as in the case in which the octahedral site was initially occupied by Al^{3+}, followed by substitution by the above metal ions at that site. In each case the cluster was totally optimized. The initial configuration of one of the clusters is shown in Figure 2. The variation of the orientation and other geometric parameters of the hydroxyl hydrogen attached to the octahedral site was monitored. As we have seen earlier, there are two different aluminums present in the dioctahedral smectites with different geometric parameters.[43] The substitution energy was calculated for the most active aluminum between the two, by the equation mentioned in Computational Methodology and Model section. The substitution energy shows that the preference

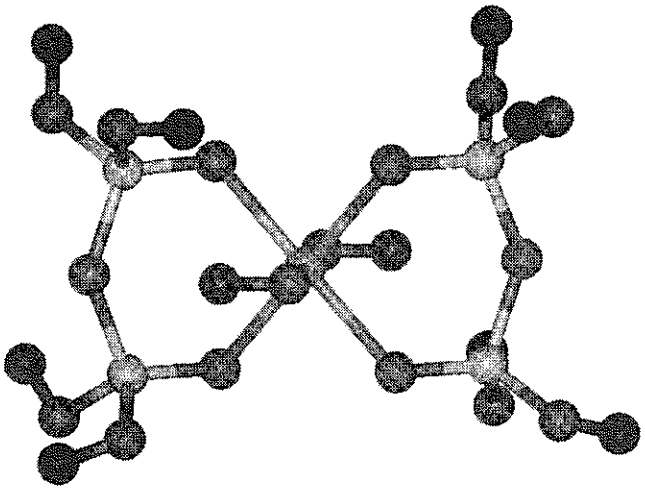

Figure 2. Initial configuration of a clay cluster having the formula $TSi_4O_{16}H_{10}$. Here T is aluminum. The color code is as follows: red, oxygen; yellow, silicon; violet, octahedral aluminum; blue, hydroxyl hydrogen; black, hydrogen at the nearest position of silicon.

TABLE 1: Optimized Geometries[a] of a 2,3,7,8-TCDD Molecule from DFT Results in Comparison to Experiment[b] and ab Initio RHF Results[c]

parameter	experiment	RHF	DFT
a(f,k,p)	1.379	1.385	1.375
b(g,l,q)	1.377	1.375	1.378
c(h,m,r)	1.384	1.384	1.382
d(i,n,s)	1.728	1.791	1.725
e(j,o.t)	1.010	1.069	1.068
u(w)	1.387	1.383	1.385
v(x)	1.385	1.380	1.386
ab(fg,kl,pq)	117.6	118.7	117.9
bc(gh,lm,qr)	121.0	119.4	120.8
cd(hi,mn,rs)	118.9	117.9	118.9
be(gj,lo,qt)	119.0	119.5	119.3
au(fw,kw,pu)	122.2	120.7	121.9
ak(fp)	115.7	116.8	115.9

[a] Refer to Figure 3 for definitions of parameters; e.g., a = bond length (Å), ab = bond angle (deg). [b] From ref 46. [c] From ref 12.

TABLE 2: Condensed Local Softness and Fukui Function Values (in Atomic Units) for 2,3,7,8-TCDD Using the ESP Technique with DFT

	ESP technique			ESP technique	
atom	f_x^-	s_x^-	atom	f_x^-	s_x^-
C1	0.021	0.085	C12	0.022	0.089
C2	0.021	0.085	C13	0.022	0.089
C3	0.030	0.122	C14	0.030	0.122
C4	0.024	0.098	Cl15	0.112	0.457
C5	0.024	0.098	Cl16	0.111	0.453
C6	0.030	0.122	H17	0.037	0.151
O7	0.0510	0.208	H18	0.037	0.151
C8	0.024	0.098	H19	0.037	0.151
C9	0.024	0.098	Cl20	0.111	0.453
O10	0.052	0.212	Cl21	0.111	0.453
C11	0.029	0.118	H22	0.037	0.151

is in iron (Fe^{3+}). The ordering of substitution follows the order $Fe^{3+} > Mg^{2+} > Fe^{2+} > Li^+$. It is noted below that the magnitude of electron density (numbers in parentheses) transferred to the metal ion is Al^{3+} (2.56) > Fe^{3+} (2.09) > Mg^{2+} (1.52) > Fe^{2+} (1.28) > Li^+ (0.06). Thus, rather than the formal charges associated with the various cations, the calculated in situ net charges are given by 0.44+, 0.91+, 0.48+, 0.72+, and 0.94+, where the same cation order as in the above set of inequalities has been kept. This ordering agrees with the proposal of Goldschmidt.[45] His proposal was based on the approximate relative sizes of metal ions in their appropriate

TABLE 3: Nonlocal Density Functional (NLDF) Study of the $AlSi_4O_{16}H_{10}$ Cluster to Calculate the Substitution Energy for Different Substituents in Place of Octahedral Al^{3+}

substituent metal ion	substituted cluster	substitution energy (eV)
Li^+	$[LiSi_4O_{16}H_{10}]^{2-}$	−12.59
Mg^{2+}	$[MgSi_4O_{16}H_{10}]^-$	−12.75
Fe^{2+}	$[FeSi_4O_{16}H_{10}]^-$	−12.68
Fe^{3+}	$[FeSi_4O_{16}H_{10}]$	−12.86

TABLE 4: Global Softness Values (in au) for Clay Clusters $[AlSi_4O_{16}H_{10}]$ with Different Isomorphously Substituted Octahedral Cations (in Place of Al^{3+}) and 2,3,7,8-TCDD Molecule

molecule	global softness (au)	molecule	global softness (au)
$[LiSi_4O_{16}H_{10}]^{2-}$	1.862 91	$[FeSi_4O_{16}H_{10}]$	1.288 99
$[MgSi_4O_{16}H_{10}]^-$	1.521 73	2,3,7,8-TCDD	4.088 04
$[FeSi_4O_{16}H_{10}]^-$	1.467 32		

valences. The results partially are in agreement with the stability order proposed by Arnowitz et al. for isomorphous substitution clays using a self-consistent charge-extended Huckel program.[46] It is observed that insertion of Li^+ in place of Al^{3+} in the octahedral layer is the least favorable process.

Now, as we have mentioned in our earlier paper,[43] the orientation of the hydroxyl hydrogen attached to the octahedral aluminum or the isomorphously substituted cation plays a crucial role in its acidity and activity. Hence, we calculated the Fukui function (f_x^+) and local atomic softness (s_x^+) for the constituent atoms of the isomorphously substituted clusters by ESP charges obtained from DFT and tabulated the results in Table 5. The results show that the activity order is different from that of the order predicted by the substitution energy. The substitution energy results predicted that Fe^{3+} results in the most stability, but when we try to monitor the activity of the hydroxyl group attached to the octahedral cation, we get a different scenario. In a situation with Mg^{2+} as the isomorphous substituent, the hydroxyl hydrogen shows the most electrophilicity, as shown in Table 5. In terms of the activity of the hydroxyl group, the order is $Mg^{2+} > Fe^{2+} > Fe^{3+} > Li^+$. To resolve the ambiguity, we calculated the geometric parameters for all of the optimized structures of isomorphously substituted clusters and an explanation is generated. It is observed that the geometry of the active site is affected with the nature of the cation present in the octahedral site substituting aluminum. The variation of the

TABLE 5: Condensed Local Softness and Fukui Function Values for Clay Clusters with Different Isomorphous Substitutions by the ESP Technique Using DFT

	substituent cation for octahedral Al^{3+}							
	Mg^{2+}		Fe^{3+}		Fe^{2+}		Li^{+}	
atom	f_x^+	s_x^+	f_x^+	s_x^+	f_x^+	s_x^+	f_x^+	s_x^+
T1	0.150	0.229	0.221	0.284	0.144	0.212	0.097	0.180
Si2	0.058	0.089	0.093	0.120	0.049	0.073	0.040	0.074
Si3	0.060	0.092	0.088	0.113	0.051	0.075	0.045	0.083
Si4	0.063	0.097	0.098	0.126	0.053	0.079	0.046	0.085
Si5	0.053	0.082	0.076	0.098	0.048	0.071	0.044	0.081
O6	0.054	0.083	0.059	0.076	0.051	0.075	0.043	0.080
O7	0.060	0.092	0.072	0.093	0.059	0.087	0.045	0.083
O8	0.064	0.098	0.065	0.084	0.055	0.082	0.043	0.080
O9	0.063	0.097	0.104	0.134	0.055	0.081	0.042	0.078
O10	0.061	0.093	0.087	0.112	0.055	0.081	0.041	0.076
O11	0.051	0.078	0.093	0.119	0.056	0.083	0.044	0.081
O12	0.052	0.079	0.069	0.088	0.060	0.089	0.040	0.074
O13	0.053	0.081	0.097	0.125	0.057	0.084	0.041	0.076
O14	0.057	0.087	0.084	0.108	0.050	0.074	0.042	0.078
O15	0.054	0.083	0.123	0.159	0.053	0.079	0.046	0.085
O16	0.064	0.098	0.078	0.100	0.057	0.085	0.040	0.074
O17	0.061	0.093	0.106	0.136	0.059	0.087	0.041	0.076
O18	0.052	0.079	0.079	0.101	0.049	0.072	0.044	0.081
O19	0.047	0.073	0.055	0.070	0.053	0.078	0.040	0.074
O20	**0.402**	**0.612**	**0.275**	**0.354**	**0.325**	**0.478**	**0.124**	**0.231**
O21	**0.458**	**0.698**	**0.348**	**0.448**	**0.370**	**0.543**	**0.149**	**0.277**
H22	0.016	0.025	0.015	0.019	0.012	0.018	0.010	0.018
H23	0.012	0.019	0.010	0.013	0.013	0.020	0.010	0.018
H24	0.013	0.021	0.017	0.021	0.014	0.021	0.011	0.020
H25	0.015	0.024	0.012	0.015	0.015	0.023	0.012	0.021
H26	0.013	0.021	0.011	0.014	0.012	0.019	0.011	0.020
H27	0.013	0.020	0.014	0.018	0.012	0.019	0.012	0.021
H28	0.011	0.018	0.018	0.023	0.013	0.020	0.011	0.020
H29	0.011	0.018	0.017	0.021	0.012	0.019	0.010	0.018
H30	**0.323**	**0.492**	**0.335**	**0.432**	**0.314**	**0.462**	**0.211**	**0.393**
H31	**0.396**	**0.603**	**0.428**	**0.551**	**0.400**	**0.587**	**0.233**	**0.434**

TABLE 6: H−O−T Bond Angles for Clay Cluster Models with Different Isomorphous Substituent Cations

clay cluster	H−O−T	clay cluster	H−O−T
$[LiSi_4O_{16}H_{10}]^{2-}$	90.78	$[FeSi_4O_{16}H_{10}]^{-}$	102.21
$[MgSi_4O_{16}H_{10}]^{-}$	102.78	$[FeSi_4O_{16}H_{10}]$	101.97

H−O−T angle for each substituted situation is tabulated in Table 6. The result shows that the activity order as predicted from the Fukui function is explainable. We monitored the H−O−T angle to account for the activity of the hydroxyl hydrogen attached with the octahedral cation because the activity of the hydroxyl hydrogen is dependent on its environment and orientation. This means that the availability of the hydroxyl hydrogen attached to the octahedral magnesium is the maximum, or in another way it will be the most active in comparison to the other isomorphic substituent. The substitution energy order shows that in the case of Fe^{3+} the structure gets most stabilized energetically which may be for many other reasons, as shown in our earlier study.[43] However, the situation with the sorbent is when the interacting molecule will be attracted by a moiety of active interaction favoring the sorption process; the interacting molecule should pave its way through the hexagonal hole resulting from the six silicons on the clay surface and will approach the most electrophilic site of the clay surface. Or in another way the most nucleophilic site of 2,3,7,8-TCDD will interact with the most electrophilic site of the clay surface, assuming that none of the tetrahedral silicons present on the clay surface layer are substituted by tetrahedral aluminum to generate some surface acidity. The specific interaction of the molecule with the clay surface will be discussed in the following sections.

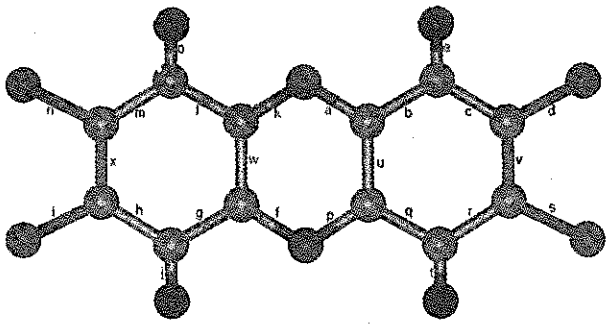

Figure 3. Structure of a 2,3,7,8-TCDD molecule and its bonding notation. Refer to Table 1 for definition of the structural parameters of the TCDD molecule. The color code is as follows: red, oxygen; green, carbon; indigo, chlorine; black, hydrogen.

b. Structure, Energy, and Reactivity Index of 2,3,7,8-TCDD. The geometry and its notation for the TCDD structure are shown in Figure 3. The optimized structural data for dioxin of DFT calculations are presented in Table 1. The total energy of TCDD is −2450.870 03 au. The geometrical parameters of TCDD, determined experimentally from an X-ray crystallographic study,[47] are also listed in Table 1. The results of Fujii et al.[12] were also compared. The results show that our calculation methodology gives the best agreement with the experimental geometries. Compared with the experimental results, the RHF/6-31G calculations severely overestimate the C−Cl bond length by as much as 0.065 Å.[12] Our DFT calculations with a polarized basis set improved the results even more than RHF/6-31G*.[12] The discrepancy of the C−O bond distance as obtained by Fujii et al.[12] compared to the experimental value is also improved.

The Fukui functions (f_x^-) and atomic local softnesses (s_x^-) are calculated using the ESP method with DFT, and the results are shown in Table 2. The results show that the most nucleophilic site of the 2,3,7,8-TCDD molecule is the chlorine atom attached, and it is more active than the oxygens present in the ring.

c. Reactivity Index Scale. The aim of the current study is to rationalize an understanding to choose a sorbent material from the dioctahedral smectite family for highly toxic dioxin. We make one approximation, by cutting down the probable candidate to only one member of the family (montmorillonite) and keeping in mind its natural availability. It is observed that 2,3,7,8-TCDD has a higher global softness value in comparison to interacting clay clusters with different isomorphous substitutions. The order of global softness of different isomorphously substituted clay clusters with respect to that of 2,3,7,8-TCDD is as follows:

$$Li^+ > Mg^{2+} > Fe^{2+} > Fe^{3+}$$

Now, we present the results of condensed local softnesses and Fukui functions of the most electrophilic atom of the cluster models with different isomorphous substitutions from ESP techniques in Table 5. The results show that in terms of both Fukui functions and condensed local softnesses the hydroxyl hydrogen attached to different octahderal cations through an oxygen bridge in an interacting clay cluster can be arranged in the order $Mg^{2+} > Fe^{2+} > Fe^{3+} > Li^+$. Here we propose a scale of activity of clay material of the 2:1 smectite family having isomorphous substituents in the octahdral cation position to locate the most active material for dioxin sorption. These results derive a scale of activity in terms of acting as sorbent for TCDD. To verify the proposed order, we perform the interaction energy calculations, which is described in the following paragraphs.

TABLE 7: BLYP and MP2 Binding Energy Results for H_2O-H_2O and H_2O-HF Using a Similar Basis Set [6-31++G(d,p)] for MP2 and DNP for BLYP

	MP2		BLYP	
system	BE[a] (kcal/mol)	BE(BSSE) (kcal/mol)	BE (kcal/mol)	BE(BSSE) (kcal/mol)
H_2O-H_2O[b]	−5.24	−4.47	−5.01	−4.54
H_2O-HF[c]	−10.15	−8.13	−9.98	−8.76

[a] BE = binding energy, BE(BSSE) = BSSE-corrected binding energy. [b] Results in ref 39. [c] Results in ref 48.

d. Interaction of Clay Clusters with 2,3,7,8-TCDD. The interaction energy calculation was performed using DFT with the BLYP functional. The validity of the current methodology in predicting the interaction energy is tested with a small model calculation with H_2O-H_2O and H_2O-HF systems. The results are compared with existing results using MP2 level calculations.[39,48] The results are tabulated in Table 7. It shows that our current methodology can reproduce the binding energy of the smaller models in comparison to the more accurate MP2 level with an error of ±0.01 kcal/mol. The clay clusters are fixed at their respective optimized structures, and the 2,3,7,8-TCDD molecule is optimized. For each case, the most nucleophilic atom (as observed from the reactive index values) of the interacting molecule was placed at a distance of 2.5 Å from the hydroxyl hydrogen attached to the octahedral cation of the clay cluster acting as the electrophilic center. Here we also made an approximation regarding the initial configuration of the TCDD. We have considered two possible initial configurations for TCDD: (1) the chlorine of TCDD pointing to the hydroxyl hydrogen and (2) the oxygen of the ring pointing to the hydroxyl hydrogen. This has been done with reference to the work of Fujii et al.[12] They mentioned the butterflylike movement of the dioxin molecule along the central benzene ring containing two oxygens. This means that while interacting with the clay surface, there will not be other possibilities of interaction. The minimum energy conformer comes from the optimization starting with the first configuration. In the optimized structure it is easily recognized that the dioxin molecule moves closer to the electrophilic site and the distance between the nucleophilic and electrophilic atom varies with the affinity. The orientations of the TCDD with respect to the clay cluster for the best situation are shown in Figure 4. The results of the total energy of the individual framework clusters and the interacting molecules along with the adsorption complex and the interaction energy (BSSE corrected) of the cases are shown in Table 8. The interaction energy values fall in the range of 3.34−9.73 kcal/mol. We will not emphasize the numbers but rather we will analyze the trend. The interaction energy values show the order with respect to the sorption of TCDD. The result matches the order predicted in terms of reactivity index values. This also validates our earlier proposition[30] that the reactivity index scale is nice for unit site interaction, i.e., the interaction of the most nucleophilic site with the most electrophilic site. Our earlier proposition, which is for zeolites, shows that the scale also is true for clays. So, from the DFT-based local parameter, one can conclusively locate the active site and hence the best material for a particular reaction; here the interacting species is TCDD. This is a novel way which will solve the immense difficulty associated with handling poisonous species such as dioxin and will get rid of the tedious experimentation needed for material designing.

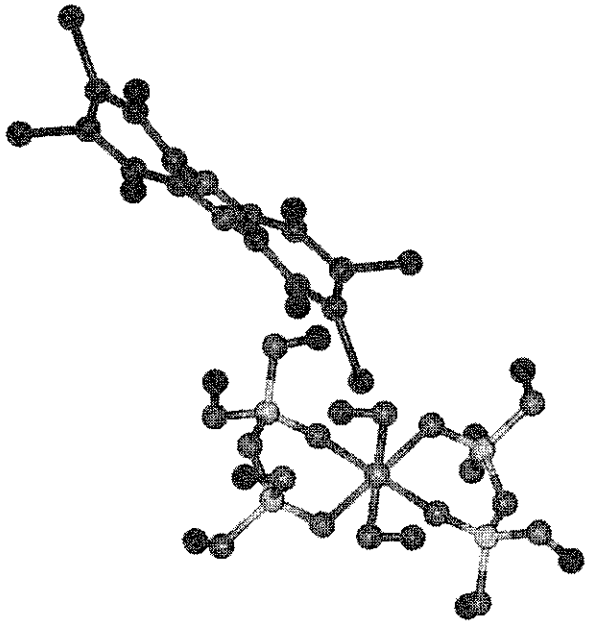

Figure 4. Optimized structure of a 2,3,7,8-TCDD molecule during interaction with a clay cluster with Mg^{2+} present as the isomorphous substituent at the octahedral alumium position. The color code is as follows: red, oxygen; yellow, silicon; violet, octahedral magnesium; blue, hydroxyl hydrogen; black, other hydrogen; green, carbon; indigo, chlorine.

TABLE 8: Total Energy of the Clay Clusters with Different Isomorphous Substituent Cations and Interacting Molecule along with Interaction Energy for the Molecule with Each of the Clay Clusters at the Optimized Geometry of the Molecule

molecule	total energy (au)	interaction energy (kcal/mol) BSSE corrected
TCDD	−2450.8700	
$[LiSi_4O_{14}H_{10}]^{2-}$	−3586.1736	
$[MgSi_4O_{14}H_{10}]^{-}$	−3602.8717	
$[FeSi_4O_{14}H_{10}]^{-}$	−3619.1765	
$[FeSi_4O_{14}H_{10}]$	−3632.5098	
TCDD + $[LiSi_4O_{14}H_{10}]^{2-}$	−6037.0489	−3.34
TCDD + $[MgSi_4O_{14}H_{10}]^{-}$	−6053.7572	−9.73
TCDD + $[FeSi_4O_{14}H_{10}]^{-}$	−6070.0582	−7.92
TCDD + $[FeSi_4O_{14}H_{10}]$	−6083.3875	−4.83

Conclusions

This is the first theoretical study to design a suitable inorganic sorbent material economically and environmentally viable for the effective sorption of highly hazardous dioxin. This study also aims to rationalize an understanding between the sorption of an organic molecule with a clay surface with respect to the hydroxyl hydrogen connected with the octahedral moiety of the framework with different isomorphous substitutions at its octahedral layer. The variation of charge in the octahedral layer influences the activity of the clay family of 2:1 dioctahedral smectite. We validate a reactivity index scale proposed by us before and extrapolated that scale to another branch of inorganic material. We have shown here the flexibility of the dioxin molecule, which paves a way to explore mesoporous material suitable for sorption of dioxin. Even in some cases the pillared clays are suitable for the same, with the pillars being the cations involved in this study. This study for the first time validated the reactivity index proposition through interaction energy calculations. The optimized geometry vividly shows pseudo bond formation between nucleophilic and electrophilic moieties

in the helm of the HSAB principle. The optimistic results pave the way for expanding the methodology for other systems as well as validation of the proposal by experimentation.

References and Notes

(1) Bumb, R. R.; Crummett, W. B.; Cutie, S. S.; Gledhill, J. R.; Hummel, R. H.; Kagel, R. O.; Lamparski, L. L.; Luoma, E. V.; Miller, D. L.; Nestrick, T. J.; Shadoff, L. A.; Stehl, R. H.; Woods, J. S. *Science* **1980**, *210*, 385.

(2) Karasek, F. W.; Onuska, F. I. *Anal. Chem.* **1982**, *54*, 309A.

(3) Travis, C. A.; Hattemer-frey, H. A. *Chemosphere* **1990**, *20*, 729.

(4) Kimbrough, R. D. *Arch. Environ. Health* **1972**, *25*, 125.

(5) Aitio, A.; Hesso, A.; Luotamo, M.; Rosenberg, C. *Chemosphere* (Special Issue on Chlorinated Dioxins and Related Compounds) **1993**, *27*, 516.

(6) Reddy, V. V.; Patterson, D. G., Jr.; Grainger, G. *Chemosphere* **1989**, *18*, 1.

(7) Makino, M.; Kamiya, M.; Matsushita, H. *Chemosphere* **1992**, *24*, 291.

(8) Koester, C. J.; Hites, R. A. *Chemosphere* **1988**, *17*, 2355.

(9) Cheney, B. V.; Tolly, T. *Int. J. Quantum Chem.* **1979**, *16*, 87.

(10) Schaefer, T.; Sebastian, R. *THEOCHEM* **1990**, *204*, 41.

(11) McKinny, J. D.; Chae, K.; McConnell, E. E.; Birnbaum, L. S. *Environ. Health Perspect.* **1985**, *60*, 57.

(12) Fujii, T.; Tanaka, K.; Tokiwa, H.; Soma, Y. *J. Phys. Chem.* **1996**, *100*, 4810.

(13) Jackson, D. R.; Roulier, M. H.; Grotta, H. M.; Rust, S. W.; Warner, J. S. In *Chlorinated Dioxins and Dibenzofurans in Perspective*; Rappe, C., Choudary, G., Keith, I. H., Eds.; Lewis Publishers: Chelsea, MI, 1986; pp 185−200.

(14) Weber, W. J., Jr.; Voice, T. C.; Pibazari, M.; Hunt, G. E.; Ulanoff, D. M. *Water Res.* **1983**, *10*, 1443.

(15) Karickhoff, S. W.; Brown, D. S.; Scott, T. A. *Water Res.* **1979**, *13*, 241.

(16) Srinivasan, K. R.; Fogler, H. S. In *Chlorinated Dioxins and Dibenzofurans in Perspective*, Rappe, C., Choudary, G., Keith, I. H., Eds.; Lewis Publishers: Chelsea, MI, 1986; pp 519−530.

(17) Srinivasan, K. R.; Fogler, H. S.; Gulari, E.; Nolan, T.; Schultz, J. S. *Environ. Prog.* **1985**, *4*, 239.

(18) Boyd, S. A.; Mortland, M. M. *Nature* **1985**, *316*, 532.

(19) Bailey, S. W. *Am. Mineral.* **1975**, *60*, 175.

(20) Sposito, G.; Prost, R. *Chem. Rev.* **1982**, *82*, 553.

(21) Delville, A. *Langmuir* **1991**, *7*, 547.

(22) Giese, R. F. *Nature* **1973**, *241*, 151.

(23) Pearson, R. G. *J. Am. Chem. Soc.* **1983**, *105*, 7512.

(24) Pearson, R. G. *J. Chem. Educ.* **1987**, *64*, 561.

(25) Parr, R. G.; Yang, W. *J. Am. Chem. Soc.* **1984**, *106*, 4049.

(26) Langenaeker, W.; Demel, K.; Geerlings, P. *J. Mol. Struct. (THEOCHEM)* **1992**, *259*, 317.

(27) Langenaeker, W.; Proft, F. De.; Geerlings, P. *J. Phys. Chem.* **1995**, *99*, 6624.

(28) Langenaeker, W.; Proft, F. De.; Geerlings, P. *J. Phys. Chem. A* **1998**, *102*, 5944.

(29) Chandra, A. K.; Geerlings, P.; Nguyen, M. T. *J. Org. Chem.* **1997**, *62*, 6419.

(30) Chatterjee, A.; Iwasaki, T.; Ebina, T. *J. Phys. Chem. A* **1999**, *103*, 2489 and references therein.

(31) Gazquez, J. L.; Mendez, F. *J. Phys. Chem.* **1994**, *98*, 4591.

(32) Yang, W.; Mortier, M. J. *J. Am. Chem. Soc.* **1986**, *108*, 5708.

(33) Pearson, R. G.; Parr, R. G. *J. Am. Chem. Soc.* **1983**, *105*, 7512.

(34) Kohn, W.; Sham, L. J. *Phys. Rev. A* **1965**, *140*, 1133.

(35) Becke, A. *J. Chem. Phys.* **1988**, *88*, 2547.

(36) Lee, C.; Yang, W.; Parr, R. G. *Phys. Rev. B* **1988**, *37*, 786.

(37) Bock, C. W.; Trachtman, M. *J. Phys. Chem.* **1994**, *98*, 95.

(38) (a) Sim, F.; St-Amant, A.; Papai, I.; Salahub, D. R. *J. Am. Chem. Soc.* **1992**, *114*, 4391. (b) Kim, K.; Jordan, K. D. *J. Phys. Chem.* **1994**, *98*, 10089.

(39) Chandra, A. K.; Nguyen, M. T. *Chem. Phys.* **1998**, *232*, 299.

(40) Boys, S. F.; Bernardi, F. *Mol. Phys.* **1970**, *19*, 553.

(41) Proft, F. D.; Martin, J. M. L.; Geerlings, P. *Chem. Phys. Lett.* **1996**, *250*, 393.

(42) Geerlings, P.; Proft, F. D.; Martin, J. M. L. In *Recent Developments in Density Functional Theory; Theoretical and Computational Chemistry 5*; Seminario, S., Ed.; Elsevier: Amsterdam, The Netherlands, 1996; pp 773−780.

(43) Chatterjee, A.; Hayashi, H.; Iwasaki, T.; Ebina, T.; Torii, K. *J. Mol. Catal. A* **1998**, *136*, 195.

(44) Chatterjee, A.; Iwasaki, T.; Ebina, T.; Hayashi, H. *J. Mol. Graphics.* **1996**, 14, 302.

(45) Goldschmidt, V. M. *Skr. Nor. Vidensk.−Akad. [Kl.] 1: Mat. Naturvidensk. Kl.* **1926**.

(46) Arnowitz, S.; Coyne, L.; Lawless, J.; Rishpon, J. *Inorg. Chem.* **1982**, *21*, 3589.

(47) Boer, F. P.; Neuman, M. A.; van Remoorte, F. P.; North, P. P.; Rinn, H. W. *Adv. Chem. Ser.* **1973**, *120*, 1.

(48) Novoa, J. J.; Planas, M.; Rovira, M. C. *Chem. Phys. Lett.* **1996**, *251*, 33.